DOI: 10.1002/adem.201300236

Processing of Magnesium Porous Structures by Infiltration Casting for Biomedical Applications

By *J. Trinidad*, I. Marco, G. Arruebarrena, J. Wendt, D. Letzig, E. Sáenz de Argandoña,* and *R. Goodall*

[*] *Mr. Javier Trinidad (Corresponding-Author)*
Mechanical and Manufacturing Department, Mondragon Unibertsitatea
Loramendi 4, Arrasate-Mondragón 20500, Spain
E-mail: jtrinidad@mondragon.edu

Mr. Iñigo Marco
Mechanical and Manufacturing Department, Mondragon Unibertsitatea
Loramendi 4, Arrasate-Mondragón 20500, Spain
Department of Materials Science and Engineering, University of Sheffield
Sir Robert Hadfield Building, Mappin Street, Sheffield S1 3JD, UK
E-mail: inigo.marco@alumni.mondragon.edu

Dr. Gurutze Arruebarrena
Mechanical and Manufacturing Department, Mondragon Unibertsitatea
Loramendi 4, Arrasate-Mondragón 20500, Spain
E-mail: garruebarrena@mondragon.edu

Dr. Joachim Wendt
Magnesium Innovation Centre, Helmholtz-Zentrum Geesthacht
Max-Planck-Strasse 1, D-21502 Geesthacht, Germany
E-mail: joachim.wendt@hzg.de

Dr. Dietmar Letzig
Magnesium Innovation Centre, Helmholtz-Zentrum Geesthacht
Max-Planck-Strasse 1, D-21502 Geesthacht, Germany
E-mail: dietmar.letzig@hzg.de

Dr. Eneko Sáenz de Argandoña
Mechanical and Manufacturing Department, Mondragon Unibertsitatea
Loramendi 4, Arrasate-Mondragón 20500, Spain
E-mail: esaenzdeargan@mondragon.edu

Dr. Russell Goodall
Department of Materials Science and Engineering, University of Sheffield
Sir Robert Hadfield Building, Mappin Street, Sheffield S1 3JD, UK
E-mail: r.goodall@sheffield.ac.uk

Abstract

Magnesium and its alloys are currently considered to be a promising metallic biomaterial.

The interest in magnesium alloys arises from their biocompatibility, bioabsorbility and

especially from their mechanical properties, which are more compatible to those of human bone than the mechanical properties of other metallic biomaterials, such as stainless steel and titanium. A medical application in which magnesium is gaining interest is regenerative medicine where scaffolds are used to create tissues from cells. For its application in regenerative medicine, the scaffolds have to present a 3D open-cell structure. The main purpose of the present research is to set up the fabrication procedure necessary to manufacture porous magnesium scaffolds; for this the replication (infiltration) process has been used and adapted to process magnesium alloys, processing five different biodegradable magnesium alloys (AZ91E, WE43, ZM20, ZWM200, ZXM200).

Keywords:

Magnesium, Cellular metals, Metallic foams, Casting, Mechanical properties

1. Introduction

Metallic foams are commonly proposed for applications in aerospace and automotive industries as shock and impact energy absorbers, filters, high-temperature gaskets, silencers, flame arresters, heaters or heat exchangers[1, 2]. However, new applications are emerging nowadays in other sectors; this is the case of scaffolds for regenerative medicine.

Regenerative medicine is the branch of the medicine that encompasses the use of cells and their molecules in artificial constructs that compensate for lost or impaired body functions[3]. This aim is achieved through the generation of tissues from cells by the utilization of artificial constructs, named scaffolds. The achievement of optimal results relies in the capacity of the cells to interact with the entire material and therefore 3D open and porous structures are desired when manufacturing the scaffolds. This scaffold geometry improves the cellular

migration, the ingrowth of the new tissue, the transport of body fluid and the vascularization through the material[1, 4–10]. Different porosities and pore sizes have been used in the literature with porosities higher than 70 % being the most common[4–10] and the most used pore size being in the range of 100 to 500 μm[4–6, 9, 10].

Currently, research with biodegradable metallic materials such as Mg and its alloys[7, 8, 11-20], Fe and Fe-Mn alloys[21, 22] and W[23–25] is being carried out in the field of medicine. Magnesium is the material that is having greater impact on the scientific community because it combines the property of being both compatible with and absorbable by the human body and the property of accelerating bone regeneration[7, 8]. In fact, most of the Mg in the human body is in the skeleton, being an essential component for bone growth and maturation[26, 27]. Regarding biocompatibility, magnesium is a biocompatible metallic material representing the fourth most abundant cation in the body and the second most important, after potassium in the intracellular medium[28]. Finally, regarding its ability to be bioabsorbed, the cations generated due to corrosion in the body environment are efficiently regulated by the body[16].

Based on these advantages, magnesium foams have been already analysed in the literature for tissue regeneration[7, 8]. However, the fabrication of magnesium foams has not been widely studied and the process parameters necessary to obtain the desired porosities and pore sizes are not yet well known[29–32].

For this reason, the main objective of the present work is to define the optimal process parameters for the fabrication of magnesium foams. AZ91E and WE43 magnesium alloys (commonly used in literature for regenerative medicine analysis[7, 8, 33]) and magnesium alloys specially designed for tissue engineering by the authors of the article were used in this work. The designed alloys are based on Mg-Zn binary alloy system with small additions of other

elements (alloys based on Mg-Zn are also common in the literature for regenerative medicine[34-36]). Magnesium foams for each alloy were manufactured with different process parameters. Finally the porosity and the mechanical properties of the magnesium foams were characterised. As a final result, the replication casting process window for five different magnesium alloys is defined.

2. Experimental methods

2.1. Materials preparation

Pure Mg (99.99 wt%), pure Zn (99.99 wt%), pure Y (99.90 wt%), pure Ca (99.5 wt%) and Mg-2%Mn master alloy were used to prepare the magnesium alloys. Magnesium was melted under a protective atmosphere (Ar) and the alloying elements were added as pure elements at a melt temperature of 750 ºC. The melt was then stirred for 30 min at 200 rpm to prevent the alloying elements from settling prior to casting. Besides the ZM20, ZWM200 and ZXM200 novel alloys, AZ91E and WE43 commercial magnesium alloys were also analysed in this study. The compositions of the alloys used in this study are indicated in **table 1**.

2.2. Infiltration casting

The installation for manufacturing magnesium foams (**figure 1**) consists of a furnace, a vacuum pump and a system for supplying a protective and pressurising gas. The infiltration was carried out in a 33 millimeters diameter steel cylinder coated with boron nitride in aerosol form. First, 250-500 μm grain size NaCl was loaded (unlike some other versions of the method, the salt particles were added loose and not pre-compacted) and next a magnesium ingot was added on top of the salt. Finally the cylinder was closed using graphite gasket rings

on top and bottom. The cylinder was then introduced into a resistance furnace and heated at a rate of 20 ºC per minute, maintaining the cylinder at the process temperature for two and a half hours to assure a homogeneous temperature before the infiltration casting. During the entire procedure, the molten magnesium was under a protective atmosphere of CO_2 + 4 % SF_6 at 0.5 bar (with a lower pressure the magnesium could sublimate). After the temperature homogenization, the gas pressure was increased forcing the molten magnesium to permeate through the salt grain preform.

After the infiltration, the steel cylinder was cooled by placing it on a copper block to allow solidification to proceed from bottom to top. This strategy helps solidification shrinkage to take place outside the salt preform avoiding unwanted extra porosity and other solidification defects that could arise as a result of slow cooling and final solidification in the centre of the sample. After the cooling, the samples were removed from the steel cylinder. Distilled water with NaOH (4 g per litre to give a pH of 13) was used to dissolve the salt in order to decrease the corrosion of the magnesium during the removal of the salt.

2.3. Porosity evaluation

The porosity of the foams was obtained according to eq. (1).

$$\wp = 1 - \frac{\rho_{foam}}{\rho_{Mg}} \qquad (1)$$

Where:

$\wp$: the porosity of the foam.

ρ_{foam}: the density of the foam based on the weight and the dimension.

ρ_{Mg}: the density of bulk Mg.

2.4. Mechanical test

Uniaxial compression tests were carried out in an Instron 4206 testing machine. Tests were performed with a compression testing device. To this device was coupled a 50 mm extensometer. The tests were conducted at a strain rate of 10^{-3} s^{-1}. The samples were machined to 6 mm in diameter and 6 mm in height. Three repetitions were prepared for each material.

3. Results and Discussion

3.1. Infiltration casting process definition

Optimal infiltration casting process parameters have been defined for manufacturing foams (such as the example in **figure 2**) with each alloy. These optimal process parameters mainly depend on the castability of each alloy and on the alloy interaction with the salt. The infiltration process for all the alloys started from 0.5 bar and the pressure was raised to 3 bar over 2 minutes. Then the corresponding infiltration pressure was applied until the melt was solidified (pressure-time profiles are shown in **figure 3**).

The infiltration pressures varied between 4 bar and 6 bar for all the alloys. Lower pressures than 4 bar were not high enough to infiltrate the magnesium through the salt and higher pressures than 6 bar were found to compress the upper region of the salt preform rather than causing infiltration, creating a compact layer between the magnesium and the salt preform that was not penetrable (**figure 4**).

In terms of process pressure, three different behaviours were observed during the study. AZ91E and ZM20 magnesium alloys needed the lowest infiltration pressure for achieving sound scaffolds. For both alloys an optimal infiltration pressure of 4 bar was defined. In the case of the novel ZXM200 and ZWM200 magnesium alloys, a slightly higher pressure of 5 bar was needed. Finally the WE43 commercial alloy needed the highest pressure of all the alloys examined in this study, 6 bar.

In terms of required process temperature, two different groups were observed. AZ91E, WE43 and ZXM200 needed a temperature of 740 ºC to achieve uniform infiltration and the required porous structures. On the other hand, ZM20 and ZWM200 alloys required higher temperatures in order to improve their fluidity and infiltrate them through the salt, 750 ºC for ZM20 and 755 ºC for ZWM200.

Different parameters that yield foams with structures suitable for scaffolds are shown in **figure 5**. According to this work overall the parameters are a temperature between 740 ºC and 755 ºC and an infiltration pressure between 4 and 6 bar.

A particular feature of applying the replication process to magnesium alloys is, as mentioned above, the need to maintain a gas pressure over the melt to reduce evaporation of the metal into the system. Unlike other examples of the replication process (as described by Conde *et al.*[37]), the system is not under vacuum when the metal melts, and some gas will be trapped inside the preform (this is part of the reason why relatively high gas pressures are needed to infiltrate the foams, even though the pore size is not small compared to what can be achieved with this technique). It was found in this work that the infiltration pressure must be maintained until complete solidification of the foam has taken place. If this does not happen,

the trapped gas expands and starts bubbling through the porous structure causing large defects as it is shown in **figure 6**.

3.2. Porosity

The porosity obtained for each alloy is given in **table 2**. The lowest porosity was achieved for ZWM200 and ZXM200 alloys (30 % at 6 bar infiltration pressure) and the highest porosity was achieved for ZWM200 alloy (69 % at 5 bar infiltration pressure). For replication into a compacted preform, the preform density will closely define the foam porosity[37]. In the experiments described here, loose packing of salt will give a consistent, but relatively low, fraction of space filled, and to obtain higher porosities the fraction of the available free space that is filled must be controlled by precise selection of the infiltration conditions. The main factors influencing the porosity are the fluidity of each alloy and the infiltration casting process parameters used during infiltration. Through the present research, a range of porosities have been obtained depending on the alloy and on the manufacturing parameters.

One of the key controllable parameters influencing the achievable porosity is the infiltration pressure. As an example, **figure 7** shows the structures achieved for the ZWM200 alloy at an infiltration pressure of 6 bar and at an infiltration pressure of 5 bar, showing that as the pressure increases the amount of metal increases and the cells are more closed off from each other. The porosity achieved at an infiltration pressure of 5 bar was 69 %, while at an infiltration pressure of 6 bar it was only 30 %. It can be noted the great effect that the infiltration pressure has in the foam porosity. However, the effect of the infiltration pressure is barely detected in the AZ91E alloy which presented a similar porosity for infiltration pressures of 4 and 6 bar (**figure 8**). It should be further noted that the lowest porosities of only 30 % are very low, well below what is typically expected of a foam. A possible explanation

for such values in the replication process would be incomplete dissolution of the salt, which can become difficult at high densities as the interpore windows become small. To attempt to avoid this, water was forced to flow through the samples to promote salt dissolution, but the possibility remains that a small quantity of NaCl could be trapped in the highest density structures, reducing the apparent porosity values by a small amount.

The results demonstrate that the manufacture of magnesium foams with variable porosity through this route is possible, although there will be a lower limit, reached when the porosity decreases dramatically and the pores tend towards becoming closed. For the concerns above relating to the possibility of trapped salt within such structures, and the fact that nearly isolated pores would not be recommended for the growth and proliferation of cells in the foam, foams with porosity percentage inferior to 40 % are not considered suitable candidates for the current application.

3.3. Mechanical properties

The influence of the process parameters on the mechanical properties of the foams has also been analysed in the present work. It must be noted that the mechanical properties of the foams are directly related to the porosity achieved within them, and therefore a direct relation between the process parameters (particularly the infiltration pressure) with the porosity and mechanical properties has been observed.

Compression tests for all the Mg alloy foams manufactured under different process parameters were performed (with typical compressive stress-strain curves shown in **figure 9**). Table 2 shows the mechanical properties of all the tested scaffolds. It can be seen that there is

an inverse relationship between the achieved porosity in the scaffolds and their mechanical response; the higher the porosity the lower the mechanical properties found.

The effect of processing on mechanical properties is clearly shown in the case of the ZWM200 alloy. This Mg alloy was processed under two different infiltration pressures at 755 ºC (5 bar and 6 bar) and gave as a result very different porosities and mechanical properties. When evaluating the mechanical properties (**figure 10**), it was noticed that the yield stress of the scaffolds was 6 times bigger when processed at the highest infiltration pressure (table 2). These results, which show much bigger changes with density than would be predicted through the Gibson-Ashby equations for foam properties[38], clearly indicate the possibility to modulate the strength of the scaffolds over a wide range. The reason that the predictions are exceeded in this case is that the density change is so wide the structure is likely to be altered significantly (particularly at the high density end of the range), and the foam does not deform following the same mechanism in both forms.

Another important requirement would be strength. The ultimate tensile strength of trabecular bone ranges from 1.55 to 5.33 MPa[39], and that of cortical bone from 130 MPa to 205 MPa[40]. The yield strength of the scaffolds manufactured in the present research work ranges from 2.13 to 12.15 MPa, comparable to the trabecular bone. As shown above, this value can of course be influenced by the foam structure, principally by the density.

4. Summary

The present work describes a reliable method established for the fabrication of magnesium foams, suitable for investigation as scaffolds, by infiltration casting. The work describes the

effect of the process parameters on the porosity and properties of foam structures with five different magnesium alloys.

For the infiltration process the temperature and infiltration pressure ranges have been defined as being from 740 ºC to 755 ºC and from 4 to 6 bar respectively. The precise selection depends on the magnesium alloy to be infiltrated, and on the desired porosity. All the processes have been carried out under a protective atmosphere of CO_2 + 4 % SF_6.

Concerning the field of application under consideration, regenerative medicine and in particular resorbable bone implants, suitable porosities for this have been achieved, based on requirements defined in the literature. The lowest achieved porosity was 30 % in the case of the ZWM200 and ZXM200 magnesium alloys, which may be influenced by retained NaCl, and the highest porosity was 69 %, typical of aluminium foams processed by this method, in the case of the ZWM200 magnesium alloy. Variations in the process parameters were shown to be able to modify the porosity achieved in the final foam sample.

In terms of mechanical properties, it has been shown that the properties found in compressive tests on the magnesium foams are close to the reported mechanical properties of human bones. As modification of the infiltration process parameters affects the properties strongly, magnesium scaffolds could be designed with mechanical properties closer to the mechanical properties of trabecular or cortical bone as desired.

For the application under consideration, important aspects that must be analysed in future work are the corrosion resistance of the newly-developed magnesium alloys, and the response of cells when cultivated in these materials. According to the corrosion resistance, residual NaCl can accelerate the corrosion of the foam. For this reason, it is recommended the use of

microtomography techniques to ensure the absence of residual NaCl before the implantation of the foams.

Acknowledgements

This work was supported by the Department of Industry, Innovation, Trade and Tourism of the Basque Government through the S-PE12MU012 project.

Received: ((will be filled in by the editorial staff))
Revised: ((will be filled in by the editorial staff))
Published online: ((will be filled in by the editorial staff))

References

[1] C.E. Wen, M. Mabuchi, Y. Yamada, K. Shimojima, Y. Chino, T. Asahina. *Scripta Materialia*. **2001**, *45(10)*, 1147–1153.

[2] R. Goodall, A. Mortensen, in *Physical Metallurgy: 5th Edition*, (Eds: K. Hono, D. Laughlin), Elsevier, Amsterdam, NL **2013**, Porous Metals

[3] European Technology Platform, *NanoMedicine Nanotechnology for Health – Strategic Research Agenda*, **2006**.

[4] Y. Hu, D.W. Grainger, S.R. Winn, J.O. Hollinger. *J Biomed Mater Res*. 2002, *59*, 563–572.

[5] H. Lu, S.M. Zhang, L. Cheng, P.P. Chen, W. Zhou, J. Liu, J. Zhou. *Key Engineering Materials*, **2007**, *330-332*, 1185–1188.

[6] G. Wen, J. Wang, M. Li, X. Meng. *Key Engineering Materials*, **2007**, *330-332*, 971–974.

[7] F. Witte, H. Ulrich, M. Rudert, E. Willbold. *Journal of Biomedical Materials Research - Part A*. **2007**, *81(3)*, 748–756.

[8] F. Witte, H. Ulrich, C. Palm, E. Willbold. *Journal of Biomedical Materials Research - Part A*. **2007,** *81(3)*, 757–765.

[9] C. Wu, J. Chang, W. Zhai, S. Ni. *Journal of Materials Science: Materials in Medicine.* **2007**, *18(5)*, 857–864.

[10] H. Yoshimoto, Y.M. Shin, H. Terai, J.P. Vacanti. *Biomaterials*. **2003**, *24(12)*, 2077–2082.

[11] M.P. Staiger, A.M. Pietak, J. Huadmai, G. Dias. *Biomaterials*. **2006**, *27(9)*, 1728–1734.

[12] X. Gu, Y. Zheng, Y. Cheng, S. Zhong, T. Xi. *Biomaterials*. **2009**, *30(4)*, 484–498.

[13] X. Gu, Y. Zheng, S. Zhong, T. Xi, J. Wang, W. Wang. *Biomaterials*. **2010**, *31(6)*, 1093–1103.

[14] M.B. Kannan, R.K.S. Raman. *Biomaterials*. **2008**, *29(15)*, 2306–2314.

[15] J. Li, Y. Song, S. Zhang, C. Zhao, F. Zhang, X. Zhang, L. Cao, Q. Fan, T. Tang. *Biomaterials*. **2010**, *31(22)*, 5782–5788.

[16] Z. Li, X. Gu, S. Lou, Y. Zheng. *Biomaterials*. **2008**, *29(10)*, 1329–1344.

[17] Q. Peng, Y. Huang, L. Zhou, N. Hort, K.U. Kainer. *Biomaterials*. **2010**, *31(3)*, 398–403.

[18] F. Witte, F. Feyerabend, P. Maier, J. Fischer, M. Stormer, C. Blawert, W. Dietzel, N. Hort. *Biomaterials*. **2007**, *28(13)*, 2163–2174.

[19] F. Witte, J. Fisher, J. Nellesen, H.A. Crostack, V. Kaese, A. Pisch, F. Beckmann, H. Windhagen. *Biomaterials*. **2006**, *27*, 1013–1018.

[20] F. Witte, V. Kaese, H. Haferkamp, E. Switzer, A. Meyer-Lindenberg, C.J. Wirth CJ, H. Windhagen. *Biomaterials*. **2005**, *26*, 3557–3563.

[21] H. Hermawan, D. Dubé, D. Mantovani. *Journal of Biomedical Materials Research Part A*. **2010**, *93A(1)*, 1–11.

[22] H. Hermawan, A. Purnama, D. Dubé, J. Couet, D. Mantovani. *Acta Biomaterialia*. **2010**, *6(5)*, 1852–1860.

[23] M. Peuster, C. Fink, P. Wohlsein, M. Bruegmann, A. Gunther, V. Kaese, M. Niemeyer, H. Haferkamp, C.V. Schnakenburg. *Biomaterials*. **2003**, *24(3)*, 393–399.

[24] M. Peuster, C. Fink, C. Von Schnakenburg. *Biomaterials*. **2003**, *24(22)*, 4057–4061.

[25] M. Peuster, V. Kaese, G. Wuensch, C. Von Schnakenburg, M. Niemeyer, C. Fink, H. Haferkamp, G. Hausdorf. *Journal of Biomedical Materials Research - Part B Applied Biomaterials*. **2003**, *65(1)*, 211–216.

[26] P. Aranda, E. Planells, J. Llopis. *Ars Pharmaceutica*. **2000**, *41*, 91–100.

[27] S. Iannello, F. Belfiore. *Panminerva Medica*. **2001**, *43*, 177–209.

[28] J. Gums. *American Journal of Health-System Pharmacy*. **2004**, *61*, 1569–1576.

[29] F.W. Bach, D. Bormann, P. Wilk, R. Kucharski. in: *Cellular Metals and Polymers* (Eds: R.F. Singer, C. Körner, V. Altstädt, H. Münstedt), Trans Tech Publications, Zuerich **2005**. Production and Properties of foamed Magnesium.

[30] F.W. Bach, D. Bormann, P. Wilk. in *Cellular Metals and Metal Foaming Technology* (Eds: J. Banhart, N.A. Fleck) MIT-Verlag, Berlin **2003**, Cellular Magnesium.

[31] C.E. Wen, Y. Yamada, K. Shimojima, M. Mabuchi, M. Nakamura, T. Asahina. *Materials Science Forum*. **2000**, *350*, 359–364.

[32] Y. Yamada, K. Shimojima, Y. Sakaguchi, M. Mabuchi, M. Nakamura, T. Asahina, T. Mukai, H. Kanahashi, K. Higashi. *Journal of Materials Science Letters*. **1999**, *18(18)*, 1477–1480.

[33] A. Krause, N. von der Hoh, D. Bormann, C. Krause, F.W. Bach, H. Windhagen, A. Meyer-Lindenberg. *Journal of Materials Science*. **2010**, *45(3)*, 624–632.

[34] S. Zhang, X. Zhang, C. Zhao, J. Li, Y. Song, C. Xie, H. Tao, Y. Zhang, Y. He, Y. Jiang, Y. Bian. *Acta Biomaterialia*. **2010**, *6(2)*, 626–640.

[35] M. Jamesh, S. Kumar, T.S.N. Sankara Narayanan. *Corrosion Science*. **2011**, *53(2)*, 645–654.

[36] A.C. Hänzi, I. Gerber, M. Schinhammer, J.F. Löffler, P.J. Uggowitzer. *Acta Biomaterialia*. **2010**, *6(5)*, 1824–1833.

[37] Y. Conde, J.F. Despois, R. Goodall, A. Marmottant, L. Salvo, C. San-Marchi, A. Mortensen. *Advanced Engineering Materials*. **2006**, *8(9)*, 795–803.

[38] L. Gibson, M. Ashby. *Cellular Solids*. Cambridge Solid State Science Series. Cambridge University press **1997**.

[39] T.M. Keaveny. in *Handbook of biomaterials properties.* (Eds: J. Black, G. Hasting). Champman & Hall, London **1998,** A2.

[40] J. Currey. in *Handbook of biomaterials properties.* (Eds: J. Black, G. Hasting). Champman & Hall, London **1998,** A1.

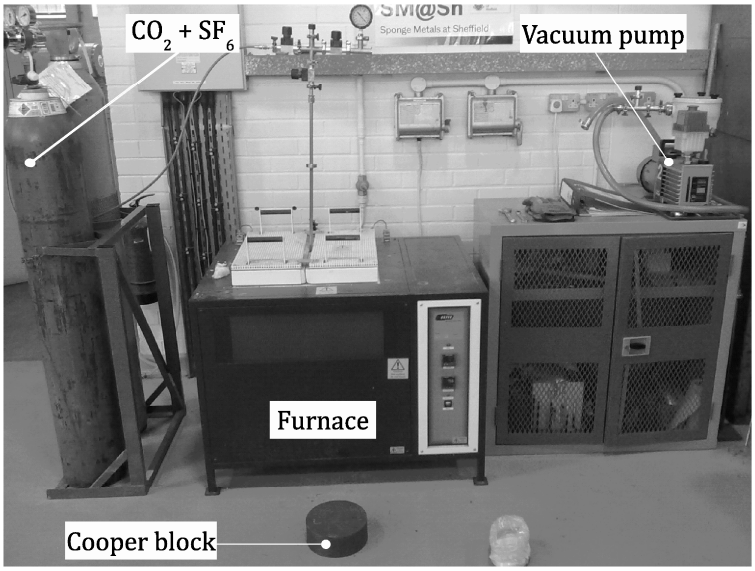

Fig. 1. Installation for foam manufacturing

Fig. 2. Sample of AZ91E foam

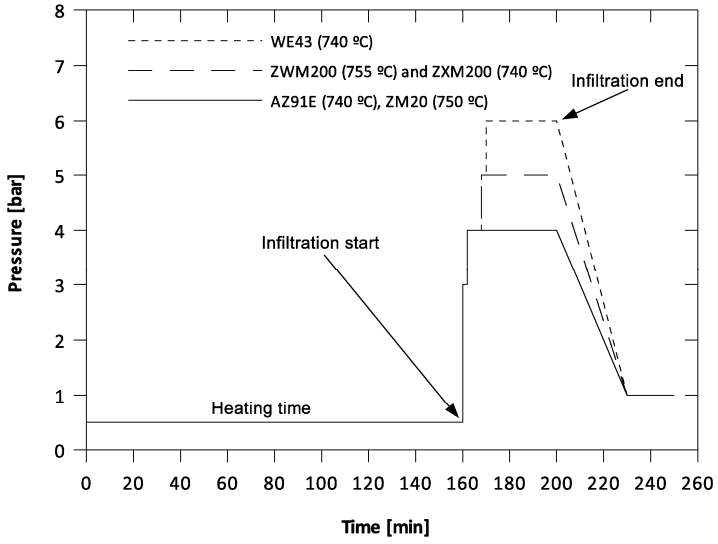

Fig. 3. Optimal infiltration pressures for maximizing the porosity while obtaining uniform infiltration in each alloy

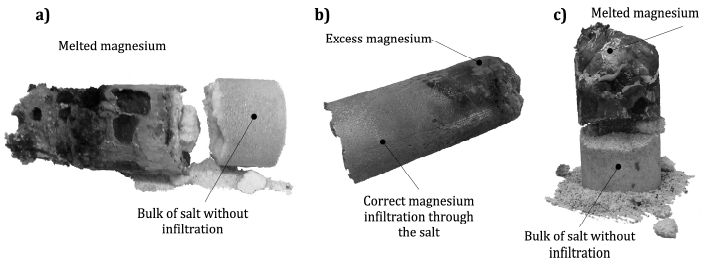

Fig. 4. AZ91E foams manufactured varying infiltration pressure. a) no infiltration under a pressure of 3 bar b) acceptable foam with infiltration pressure of 4 bar c) no infiltration due to preform compaction under a pressure of 8 bar

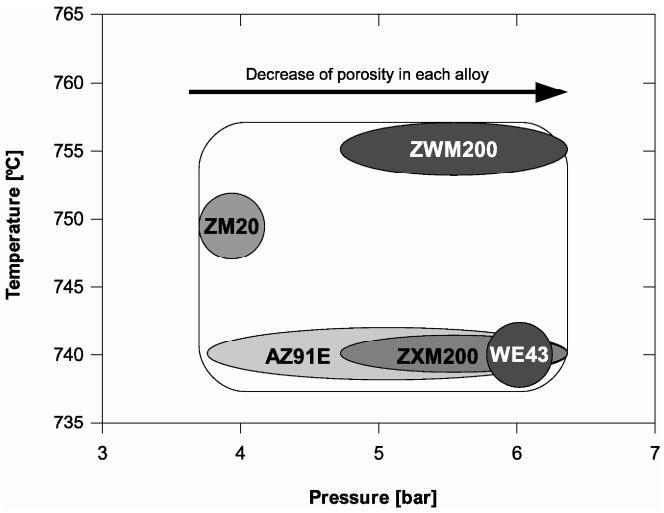

Fig. 5. Process window for the different magnesium alloys examined to produce foams with suitable structures

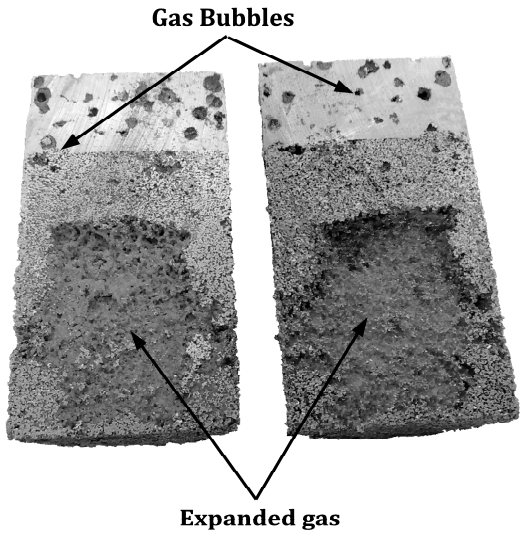

Fig. 6. Section of an AZ91E foam that was depressurized before solidification. Defects due to gas expansion and gas bubbling are shown

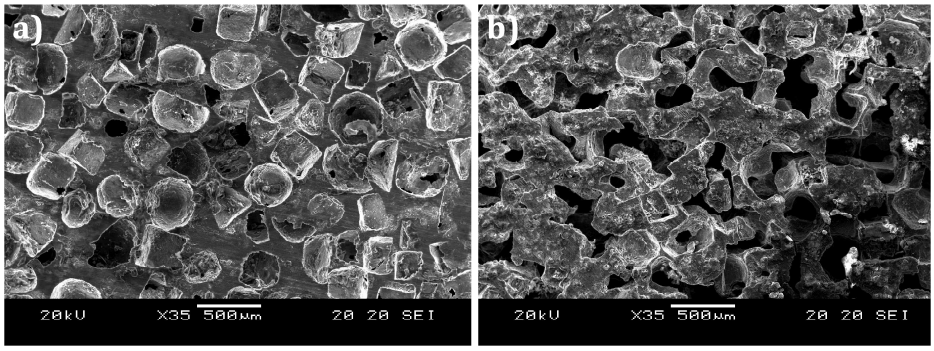

Fig. 7. Structures of ZWM200 foams with an infiltration pressure of a) 6 bar, and b) 5 bar

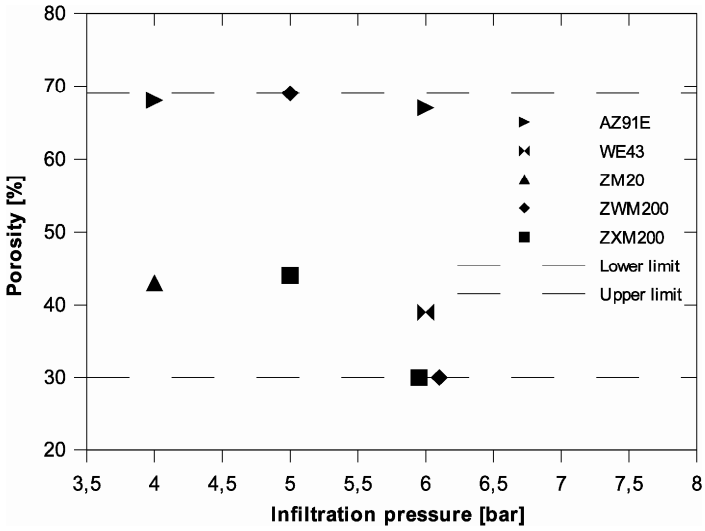

Fig. 8. Upper and lower limits of the achieved porosities for each alloy depending on the infiltration pressure

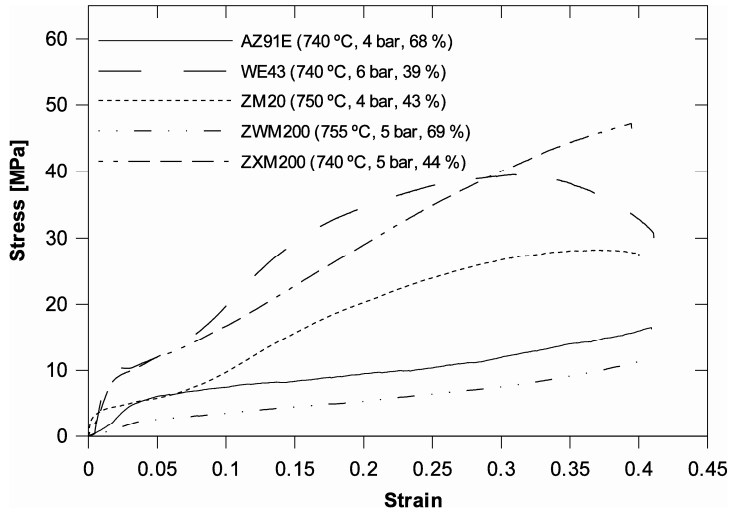

Fig. 9. Example compressive stress-strain curves for magnesium alloy foams examined in this study

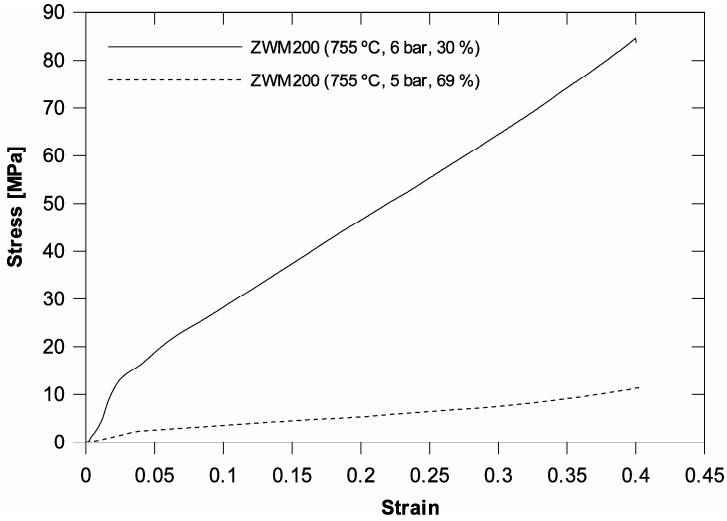

Fig. 10. Compression test stress-strain curves of the ZWM200 foams manufactured with different infiltration pressures, showing the decrease of mechanical properties of the foam with increasing porosity

Table 1. Compositions (%) of AZ91E and WE43 commercial magnesium alloys (according to ASTM B 93) and of developed magnesium alloys

	Mg	Al	Mn	Zn	Y	RE	Zr	Si	Cu	Ni	Ag	Fe	Ca
ZM20	remainder	0.0100	0.259	1.88	-	0.00150	-	0.0252	0.00107	0.00107	-	0.00315	0.00124
ZWM200	remainder	0.0215	0.238	1.97	0.532	0.00856	-	0.0123	0.00040	0.00040	0.00116	0.00136	0.00489
ZXM200	remainder	0.0165	0.220	1.88	-	0.00231	-	0.0239	0.00188	0.00188	-	0.00542	0.20
AZ91E (ASTM)	remainder	9.3-9.2	0.17-0.50	0.45-0.9	-	-	-	0.2 max	0.015 max	0.0010 max	-	0.005 max	-
WE43 (ASTM)	remainder	-	0.03 max		3.7-4.3	2.4-4.4	0.3-1.0	-	0.01 max	0.004 max	-	-	-

Table 2. Porosity, Young's modulus and Yield Stress of the magnesium alloy foams

Magnesium alloy	Infiltration temperature [ºC]	Infiltration pressure [bar]	Porosity	Yield stress [MPa]
AZ91E	740	4	68 %	3.62
	740	6	67 %	3.12
WE43	740	6	39 %	8.67
ZM20	750	4	43 %	3.48
ZWM200	755	5	69 %	2.31
	755	6	30 %	12.15
ZXM200	740	5	44 %	8.66
	740	6	30 %	9.19